Special issue of the 3rd International Conference on Computational and Experimental Science and Engineering (ICCESEN 2016)

Influence of Cu Addition and Austempering Treatment on Mechanical Properties and Microstructure of GGG 50

B. Kilinc and S. Kirtay*

Istanbul University, Engineering Faculty, Department of Metallurgical and Materials Eng., 34320 Avcilar, Istanbul, Turkey

An investigation was carried out to examine the effect of austempering on the microstructure and mechanical properties of nodular cast iron GGG 50 (DIN EN 1563) alloyed with different amount of copper. Optical, scanning electron microscopy and energy dispersive spectroscopy analyses were performed for microstructural characterization. In addition, hardness and tensile tests were carried out for mechanical properties determination. Specimens were austenitized at 900 °C for an hour, then austempered for an hour at 330 °C in salt bath and cooled at a room temperature in air. The results indicated that the addition of Cu to GGG 50 encouraged pearlite formation in the matrix structure. In addition, with the austempering heat treatment, the structure was transformed from ferrite + pearlite into ausferrite and retain austenite. Furthermore, for the alloy with 2 wt% Cu addition, it was noted that the graphite nodules diverged from sphericity and Cu was concentrated around the graphite. After austempering, mechanical properties were significantly improved and the highest mechanical properties were found at 1.5 wt% Cu.

DOI: 10.12693/APhysPolA.132.461

PACS/topics: austempering, cast iron, mechanical properties, microstructure

1. Introduction

Ductile cast irons contain 3.4–3.9% C and 1.8–3.1% Si [1]. Minor additions of Mg or Ce lead to spheroidization of graphite. Ductile cast iron can contain ausferrite (high carbon austenite+ferrite) structure by addition of Ni, Mo, and Cu together with heat treatment. This dual phase microstructure provides high strength and toughness. In this case, properties of austempered ductile cast iron (ADI) and steel become very similar. ADI is obtained by the two-stage process including austenitizing and austempering heat treatment [1, 2].

Austempering consists of heating to the austenitizing temperature, followed by quenching into a salt bath at a temperature in the range of 200 to 450 °C and holding for the time required for bainitic transformation to occur at this temperature [3].

Austempered ductile cast irons combine the high strength, elasticity [4], fracture toughness [5], resistance of fatigue [6, 7], impact resistant [8] and wear resistance [9, 10] of steel with the castability and low production cost of ductile cast iron. It also exhibits lower density compared to steel.

Mechanical properties and microstructures of ADI depend on austempering time and temperature. In literature, the effect of alloying elements (Mn, Cu, Al, Ni, Mo, Co) on the microstructure and mechanical properties of ADI [11–14] had been investigated extensively. Copper can stabilize austenite zone of the phase diagram by increasing both transformation rate during austenitizing process and the carbon content in the matrix. On the other hand, during the austempering process, copper may restrain carbide formation [11].

In literature, studies with copper additions to ADI consist of amounts between 0.1 to 1 wt% [15–18]. This work is an attempt to investigate the effect of higher content copper additions and austempering heat treatment on the microstructural changes. Mechanical properties had also been examined by adding different amount of Cu (1, 1.5, and 2 wt%) into GGG 50 grade cast iron.

2. Experimental procedure

GGG 50 grade ductile cast iron was prepared in a commercial foundry using induction melting furnace (Inductotherm) of 1500 kg capacity and sand cast in the cylindrical shape with 20 mm diameter and 190 mm length. The charge was composed of pig iron (500 kg), steel sheet (900 kg), nodular iron scrap (100 kg), sphero carbon (34 kg) and Fe–Si (30 kg). The melt was treated with FeSiMg alloy (45% Si) at 1580 °C for nodularization process. Then, it was treated with Fe–Si alloy to promote a higher nodule count and nodularity during the flow. Following this step, Cu addition was carried out in a 20 kg capacity crucible. Then the parts were cast. The spectral analysis of the cast parts are shown in Table I.

TABLE I

Spectral analysis results of samples with given Cu addition [wt%].

+Cu	C	Si	Mn	P	S	Mg	Cu
0	3.68	2.75	0.165	0.027	0.020	0.038	0.044
1	3.80	2.78	0.121	0.033	0.013	0.041	0.958
1.5	3.72	2.83	0.134	0.029	0.017	0.047	1.57
2	3.75	2.62	0.161	0.012	0.011	0.033	2.09

*corresponding author; e-mail: kirtay@istanbul.edu.tr

Samples were austenitized at 900 °C for 60 min and transferred rapidly into a salt bath (50% KNO_3 and 50% $NaNO_3$) and then held at 330 °C for 60 min and air-cooled to room temperature. Both as-cast and austempered samples were examined using standard metallographic techniques such as grinding, polishing and etching with 2% Nital solution for 4 s for optical properties investigation. Optical, scanning electron microscopy (SEM) and energy dispersive spectroscopy (EDS) analyses were carried out by Nikon optical microscope and JEOL JSM 5600 scanning electron microscope, respectively.

Rockwell C and Vickers hardness were measured by using Zwick/Roell ZHU under a load of 150 kg and 10 kg, respectively. Four measurements were made and the average values were used.

Both as-cast and austempered tensile test specimens were prepared according to ASTM standard E 8M [19]. Tensile tests were applied on specimens by using a 10 kN hydraulic testing machine (model: Losenhausen) at room temperature and ambient atmosphere with a cross-head speed of 6 mm/min. Three samples of each condition were subjected to tensile testing. The conditions were: unalloyed, 1, 1.5, and 2 wt% Cu additions with and without austempering. Thus, there were total of 24 tensile testing. Load and displacement plots were obtained on a X–Y recorder and from these load displacement diagrams yield strength and ultimate tensile strength values were calculated. The average values from three test samples are reported in this paper.

3. Results and discussions

Microstructure images of as-cast samples are given in Fig. 1. As illustrated in Fig. 1a, the specimen (unalloyed with Cu) shows a typical bull's eye structure with ferrite surrounding the graphite nodules in a pearlitic matrix.

In Fig. 1b, 1 wt% Cu added alloy consists of ferrite and pearlite. It can be seen that as the copper content was increased, pearlitic phase formation was promoted, and ferrite was transformed to pearlite. The matrix still contains a small ratio of ferrite where the spherical graphites are formed within.

Pearlite phase ratio was significantly increased and ferrite was decreased in Fig. 1c. Thus, it can be concluded that with the addition of Cu to GGG 50, the microstructure was transformed from ferrite+pearlite to pearlitic. It can be seen that the microstructure of 1.5 wt% Cu added alloy was almost completely pearlitic. Similar findings have been reported in the literature [20, 21].

By the addition of 2 wt% Cu, it can be seen in Fig. 1d that the spherical geometry of graphite was converted to flake-like structure. Hurst and Riley [22] studied different levels of copper addition to 14% silicon irons and found that higher levels of copper addition to 7%, the flake graphite become acicular in a 60° Widmanstatten structure.

The microstructure of the samples austenized at 900 °C for 1 h and austempered at 330 °C for 1 h is in Fig. 2.

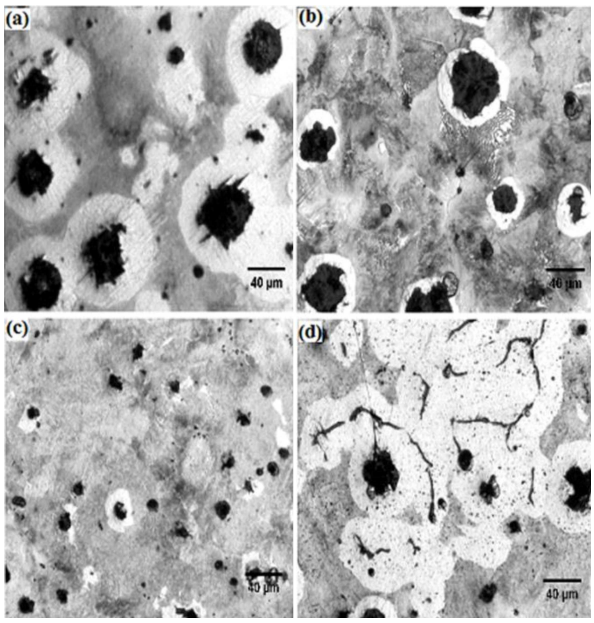

Fig. 1. Microstructure of as-cast samples: (a) unalloyed with Cu, (b) 1 wt% Cu alloyed, (c) 1.5 wt% Cu alloyed, (d) 2 wt% Cu alloyed.

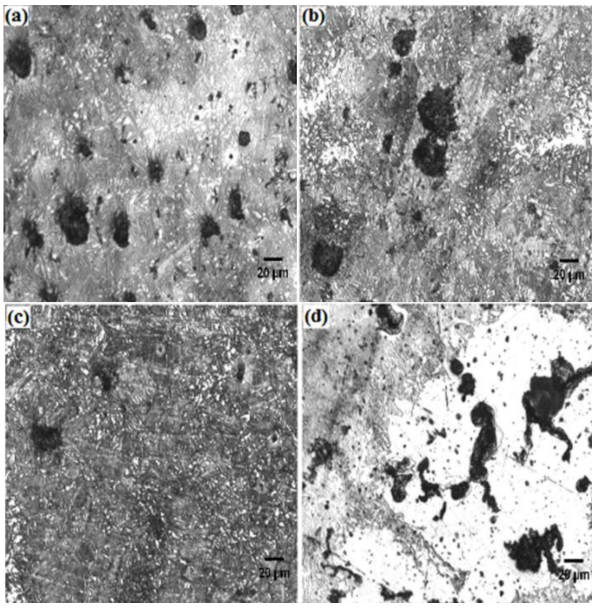

Fig. 2. Microstructures after austempering at 330 °C for an hour: (a) unalloyed with Cu, (b) 1 wt% Cu alloyed, (c) 1.5 wt% Cu alloyed, (d) 2 wt% Cu alloyed.

When closely examined, Fig. 2a–c shows that instead of ferrite and pearlite, the microstructure consists of retained austenite and ausferrite. Ausferrite is formed from bainitic ferrite + high carbon austenite. The light regions in the microstructure represents retained austenite, dark regions are bainitic ferrite and light gray regions are high carbon austenite. C, Ni, Mn, Co and Cu are well-known austenite stabilizing elements. Therefore, the addition of Cu to cast iron leads to the formation of retained austenite.

The microstructure of austempered 1 wt% Cu added alloy contains retained austenite. Similar findings have been reported in the literature related to the formation of retained austenite by the copper addition [20, 23].

In Fig. 2d, flake graphite can be seen in the microstructure of austempered 2 wt% Cu added alloy. It is important note that the spherical graphite was transformed to flake-like structure.

It can be concluded that four of the austempered microstructures look similar to each other. The matrix of the austempered samples consists of high carbon austenite and ferrite plates with retained austenite. These are formed due to the high carbon austenite and bainitic ferrite where it mainly consists of upper bainite. Literature survey results indicate that upper bainite is formed at these working temperatures [23].

Hardness measurements of as-cast and austempered GGG 50 samples were carried out as HRC and HV. These results are given as a function of Cu content in Fig. 3.

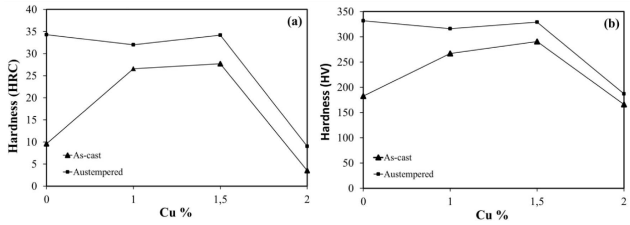

Fig. 3. Hardness changes as a function of copper content for as cast and austempered samples: (a) HRC, (b) HV.

HRC values of 2 wt% Cu added alloy for as-cast and austempered are 3.5 and 9, respectively. Readings below HRC 20 are generally considered unreliable. Therefore, the Vickers hardness test was conducted instead of HRC in order to obtain more reliable results.

Figure 3 indicates that the hardness of the austempered samples is higher than the as-cast samples. When comparing the effect of Cu addition on the hardness of as-cast samples, it can be seen that hardness increases up to 1.5 wt% Cu addition and drops after 1.5 wt% Cu addition. The hardness values of as-cast samples are 9.6, 26.6, 27.4, and 3.5 HRC. The Vickers hardness values of these samples are 182.7, 267, 290.7 and 166 HV. These corresponds to the hardness of unalloyed, 1, 1.5, and 2 wt% Cu additions, respectively. Similarly, that of austempered samples are 34.3, 32, 34.2, and 9 HRC; 332, 316, 329, and 187 HV. There was a decrease in hardness for both as-cast and austempered after 1.5 wt% Cu added samples. This can be explained by the deformation of graphite structure in the microstructure. The findings also show that for 1 and 1.5 wt% Cu added to GGG 50 alloy, the hardness of the as-cast and austempered samples can be found to be close to each other. For the hardness of austempered samples, although the hardness seems to decrease slightly at 1 wt% Cu, yet the trend of hardness appears to be unchanged regardless of the copper content. Hafiz found that as the pearlite phase ratio increases in ductile cast iron alloys, the hardness is increased. He studied the change of hardness in ductile cast iron alloys where non-alloyed as-cast samples had hardness values of as low as 9.2 HRC. By the addition of Cu and Ni, this value was increased to 21–26 HRC. By additional austempering heat treatment, 32–33 HRC values were obtained [24]. On the other hand, Neri and Cerrano [25] obtained 314 HV value when ductile cast iron alloying with 1.13% Cu. These findings are in good agreement with results obtained in this work.

In order to determine the effect of copper addition and austempering heat treatment, three samples were collected and subjected to tensile testing. The average values are given in Table II. As can be seen in Table II, for the as-cast specimens, the yield and tensile strength are increased up to 1.5 wt% Cu addition. However, after this value, it decreases significantly. For the austempered specimens, the strength values essentially do not change up to 1.5 wt% Cu. Then it decreases with Cu addition. Anil Kumar and Suresh [26] claimed that the decrease in mechanical properties for 1 wt% Cu additions were related with the decreased content of retained austenite. Gorny et al. [15] concluded that high ductility and hardenability could be achieved when Ni content was up to 2 wt% and Cu was up to 1.5 wt%.

TABLE II

Yield and tensile (right) strength [MPa] of specimens with given Cu addition [wt%].

	As-cast		Austempered	
+Cu	yield	tensile	yield	tensile
0	411	497	810	859
1	547	624	791	842
1.5	719	820	823	880
2	365	415	648	728

These results are in good agreement with regard to the hardness and microstructural analyses. It is worth noting that for the as-cast specimen with 1.5 wt% Cu addition, the mechanical test results are practically similar to those of austempered. For the unalloyed samples, the difference between the yield and tensile strength of as-cast and austempered samples is nearly twofold. On the other hand, when copper is added, the difference is not so significant.

Austempering temperature has a dominant effect over the mechanical properties since it determines the grade of ADI. When the temperature is selected to be low, finely distributed needle-like structure with low austenite levels is achieved. As a result, strength is increased but ductility is lowered. As the austempering temperature is increased, austenite ratio in the microstructure is increased and carbide formation is decreased. Therefore, elongation is increased but material suffers from decreased strength. Overall, for the required mechanical properties, appropriate selection of the temperature and holding time must be determined [27, 28]. In this work,

austenitizing temperature was selected to be 900 °C for an hour and austempering temperature was chosen as 330 °C for an hour in salt bath and samples were cooled at a room temperature in air. In this way, the finer scale microstructure was obtained and this helped to high strength of the material for 1 and 1.5 wt% Cu addition. Akca and Kinikoglu [29] reported that the main alloying elements used for raising the capacity for bainitic hardening of ductile iron were Ni, Cu, and Mo. Copper was added in quantities exceeding the limits of solid solubility in ferrous alloys ($\approx 0.7\%$) and was found to significantly improve the strength and toughness [21].

The highest hardness, yield and tensile strength were obtained in the samples where the copper addition was 1.5 wt%. SEM studies show that flake-like graphites are formed when copper content is increased to 2 wt%. SEM images are given in Fig. 4.

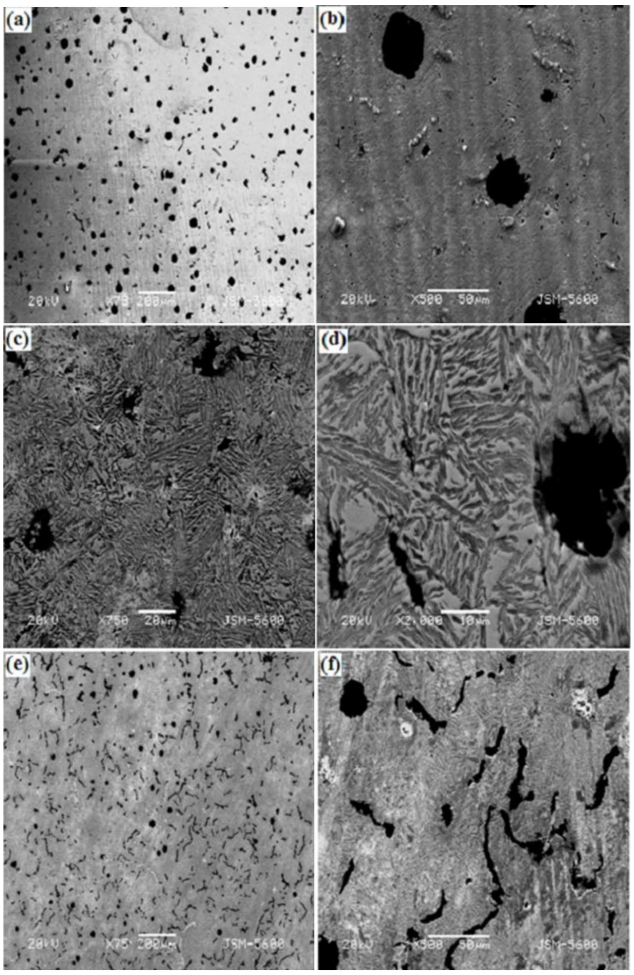

Fig. 4. SEM images of 1.5 wt% and 2 wt% Cu added specimens: (a, b) 1.5 wt% Cu alloyed, (c,d) austempered 1.5 wt% Cu alloyed, (e,f) austempered 2 wt% Cu alloyed.

In this figure, in part (a),(b), 1.5 wt% Cu added, in (c),(d) austempered 1.5 wt% Cu added, and in (e),(f), 2 wt% Cu added and austempered samples are shown. It can be seen that perlitic formation is promoted when

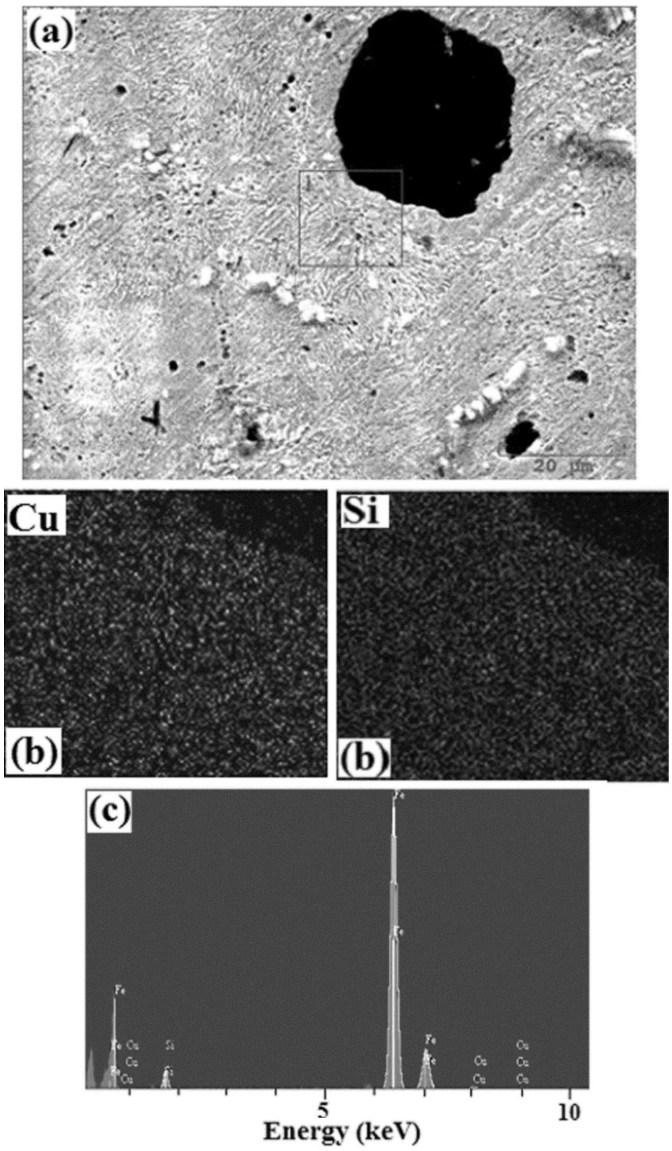

Fig. 5. (a) SEM image of the alloy containing 1.5 wt% Cu. (b) Mapping that show Cu and Si content, (c) EDS analysis.

1.5 wt% Cu is added whereas, after austempering, ausferrite and retained austenite are dominant in the microstructure. In Fig. 4d, dark colored needle-like bainitic ferrite is present together with light colored high carbon austenite. In Fig. 4e,f, SEM images of 2 wt% Cu added and austempered samples show that low grade graphites are formed as flake graphite.

For the samples where copper content is 2 wt%, the microstructural examinations show a different characteristic compared to the rest of the samples. Most of the spherical graphites are decomposed into flakes (Fig. 4e,f). This transformation results in stress concentration on sharp edges which can easily initiate cracks and thus lower mechanical properties [12].

Figure 5a shows SEM image of a sample that contains 1.5 wt% of Cu where a region has been selected. The

mapping analysis of this region given in Fig. 5b shows Cu and Si distribution. EDS result is given in Fig. 5c which reveals Fe, Cu, and Si content. It can be seen that Cu and Si are evenly and homogeneously distributed. Thus, Cu can segregate towards grain boundary. Shelton and Bonner [21] studied 1.5% added Cu and concluded that copper-rich regions are present around graphite and ausferrite.

4. Conclusions

- Cu addition to GGG 50 promotes pearlite formation in the matrix.
- After austempering heat treatment, the microstructure is transformed from ferrite + pearlite to ausferrite and retained austenite.
- Cu addition to GGG alloy is twofold: up to 1.5 wt% Cu addition, the mechanical properties increase and after 1.5 wt% Cu addition, this effect is reversed. This can be explained by the destruction of spherical graphite to flake-like structure.
- Due to the promotion of pearlitic phase, the highest hardness, yield and ultimate tensile strength values are obtained in the 1.5 wt% Cu added as-cast condition.
- Cu addition has no effect on hardness, yield and ultimate tensile strength of austempered ductile cast iron samples.

References

[1] W.F. Smith, *Structure and Properties of Engineering Alloys*, 2nd ed., McGraw-Hill, New York 1993.

[2] Y.J. Kim, H. Shin, H. Park, J.D. Lim, *Mater. Lett.* **62**, 357 (2008).

[3] Y. Tanaka, H. Kaget, *Mater. Trans.* **33**, 543 (1992).

[4] R.B. Gundlach, J.F. Janowak, *AFS Trans.* **94**, 377 (1983).

[5] K.P. Susil, *Mater. Sci. Eng. A* **297**, 31 (2001).

[6] C. Lin, P. Lai, T. Shih, *Int. J. Fatigue* **18**, 297 (1996).

[7] P. Reed, R. Thomson, J. James, D. Putman, K. Lee, S. Gunn, *Mater. Sci. Eng. A* **346**, 273 (2003).

[8] O. Eric, L. Sidjanin, Z. Miskovic, S. Zec, M. Jovanovic, *Mater. Lett.* **58**, 2707 (2004).

[9] M.J. Pérez, M.M. Cisneros, H.F. López, *Wear* 260, 879 (2006).

[10] B. Ceccarelli, R. Dommarco, R. Martinez, M. Gamba, *Wear* **256**, 49 (2004).

[11] Y. Mi, *Scr. Metall. Mater.* **32**, 1313 (1995).

[12] B.Y. Lin, E.T. Chen, T.S. Lei, *Scr. Metall. Mater.* **32**, 1363 (1995).

[13] C.H. Hsu, M.L. Chen, C.J. Hu, *Mater. Sci. Eng. A* **444**, 339 (2007).

[14] A.R. Kiani-Rashid, *J. Alloys Comp.* 474, 490 (2009).

[15] M. Gorny, E. Tyrała, H. Lopez, *J. Mater. Eng. Perform.* **23**, 3505 (2014).

[16] A.R. Mattar, S.C. Heck, A.L. Neto, F.A.P. Fernandes, G.E. Totten, L.C. Casteletti, *Int. Heat Treatm. Surf. Eng.* **5**, 78 (2011).

[17] A.M. Omran, G.T. Abdel-Jaber, M.M. Ali, *Int. J. Eng. Res. Appl.* **4**, 90 (2014).

[18] Y. Amran, A. Katsman, P. Schaaf, M. Bamberger, *Metall. Mater. Trans. B* **41**, 1052 (2010).

[19] *Standard Test Methods for Tension Testing of Metallic Materials [Metric]*, Annual Book of ASTM Standards, ASTM E8 M, Vol. 01.02, 1990.

[20] U. Seker, H. Hasirci, *J. Mater. Process. Technol.* **173**, 260 (2006).

[21] P.W. Shelton, A.A. Bonner, *J. Mater. Process. Technol.* **173**, 269 (2006).

[22] J.E. Hurst, R.V. Riley, *J. Iron Steel Inst.* **155**, 172 (1947).

[23] U. Batra, S. Ray, S.B. Prabhakar, *J. Mater. Eng. Perform.* **13**, 64 (2004).

[24] M. Hafız, *J. Mater. Sci.* **36**, 1293 (2001).

[25] M.A. Neri, C. Carreno, *Mater. Character.* **51**, 219 (2003).

[26] M.M. Anil Kumar, R. Suresh, *Int. J. Mech. Eng. Robot. Res.* **1**, 113 (2012).

[27] B. Avishan, S. Yazdani, D. Jalali Vahid, *Mater. Sci. Eng. A* **523**, 93 (2009).

[28] A.H. Elsayed, M.M. Megahed, A.A. Sadek, K.M. Abouelela, *Mater. Des.* **30**, 1866 (2009).

[29] C. Akca, N.G. Kinikoglu, *Met. Sci. Heat Treatm.* **52**, 420 (2010).